SUPPLEMETARY INFORMATION

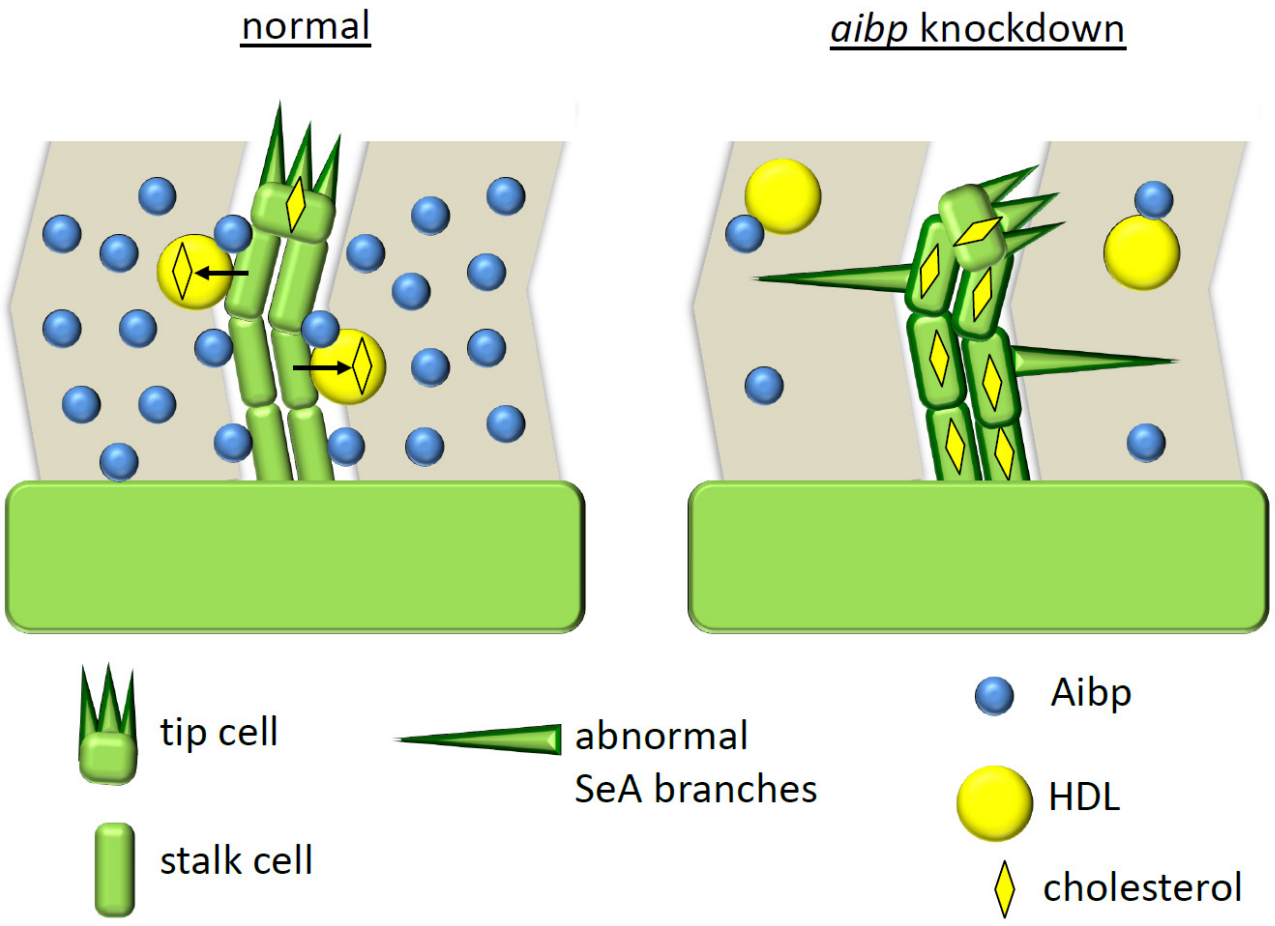

Supplementary Figure 1. Diagram illustrating the hypothesis that expression of zAibp2 in somites (tan-shaded areas) but not in the inter-somitic space accelerates cholesterol efflux from EC to HDL. Because cholesterol removal from the plasma membrane reduces lipid rafts and inhibits Vegfr2 signaling, the tip cell is guided in the direction where zAibp2 is least present. In *zaibp2* knockdown embryos, defective cholesterol efflux leads to a higher abundance of lipid rafts (depicted as dark green boundaries of EC in right-hand panel) and enhanced Vegfr2 signaling, which result in misguided growth and ectopic branching of SeA.

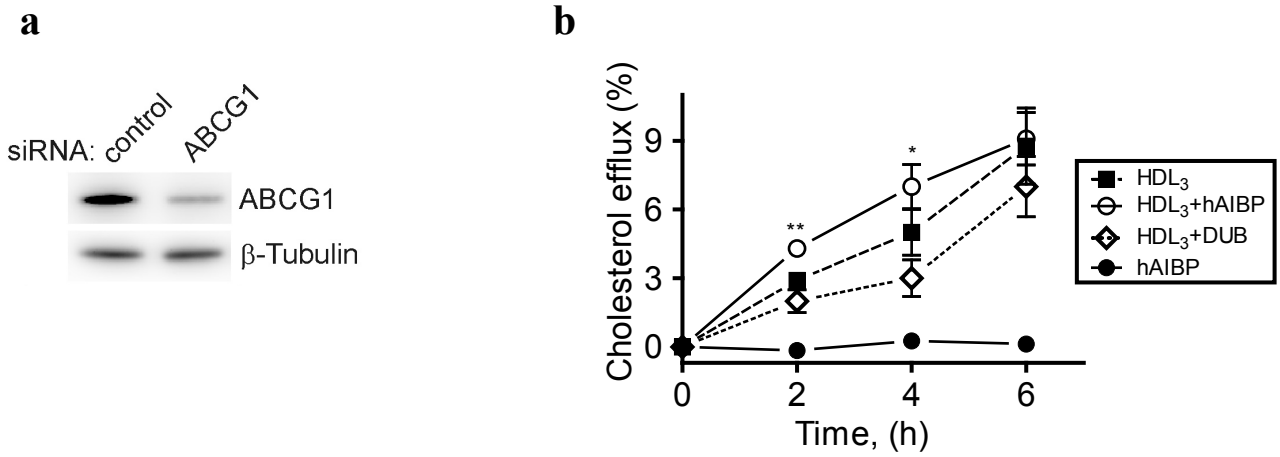

Supplementary Figure 2. a, ABCG1 knockdown in HUVEC. The blot shown in this supplementary figure confirms the ABCG1 knockdown in cells used in the experiments of Fig. 1a in the main text. **b, Kinetics of cholesterol efflux from HUVEC to HDL_3.** HUVEC were preloaded with ^3H-cholesterol and then incubated for 2, 4 or 6 hours with 50 μg/ml HDL_3 in the presence or absence of 0.2 μg/ml hAIBP or 0.2 μg/ml deubiquitinase (DUB, a non-relevant protein of the same molecular weight as hAIBP). The cholesterol efflux was measured as described in Methods. Note that hAIBP in absence of HDL_3 did not induce cholesterol efflux from HUVEC. Mean±SD; n=3. *, $p<0.05$; **, $p<0.01$.

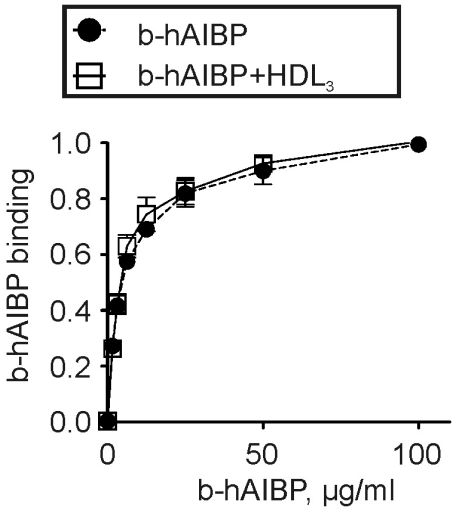

Supplementary Figure 3. hAIBP binding to HUVEC. HUVEC were incubated on ice with the indicated concentrations of biotinylated hAIBP (b-hAIBP), in the presence or absence of HDL_3 (at a 2:1 w/w hAIBP:HDL_3 ratio), and the b-hAIBP binding was determined by a chemiluminescent assay. A non-linear regression fit of both binding curves yielded $K_d = (1.1 \pm 0.4) \times 10^{-7}$ M for hAIBP/HUVEC binding.

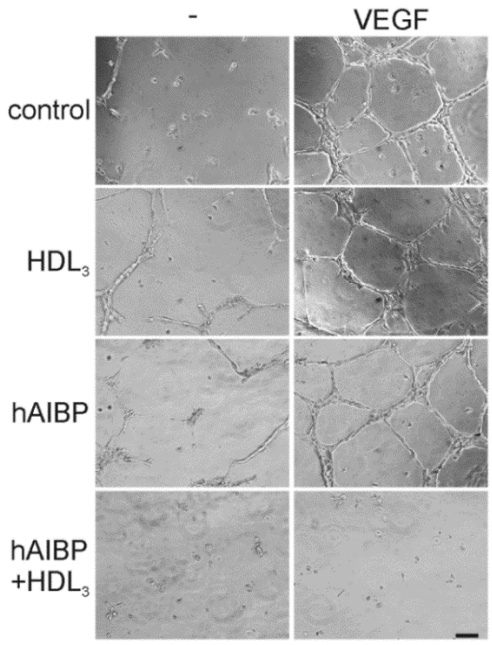

Supplementary Figure 4. Effect of hAIBP and HDL_3 on EC tube formation. This supplementary figure is an extension of Fig. 1d in the main text to illustrate the results shown on the graph of Fig. 1e. For that reason, the top and bottom row images in this supplementary figure are identical to the images in Fig. 1d. HUVEC were preincubated with 50 μg/ml HDL_3, 0.1 μg/ml hAIBP, or 50 μg/ml HDL_3 + 0.1 μg/ml hAIBP. Cells were then seeded on Matrigel, in the presence or absence of 20 ng/ml VEGF, and imaged following a 12 hour incubation.

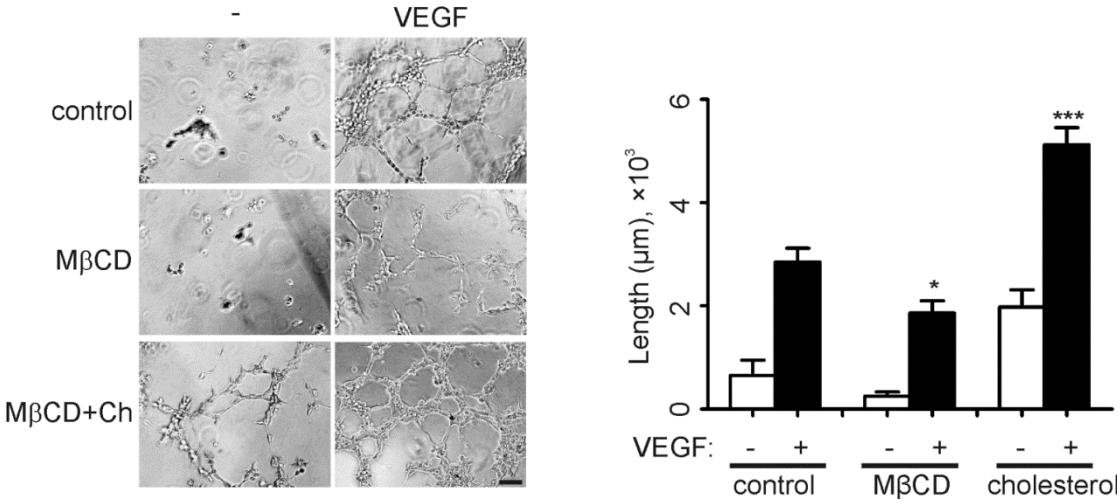

Supplementary Figure 5. Effect of MβCD and cholesterol-MβCD on EC tube formation. HUVEC were preincubated with 10 mM MβCD for 30 min or 20 μg/ml cholesterol-MβCD for 4 hours. Cells were then seeded on Matrigel, in the presence or absence of 20 ng/ml VEGF, and imaged following a 6 hour incubation. Scale, 100 μm. Mean±SD; n=3. *, $p<0.05$; ***, $p<0.001$ vs. VEGF/control.

a

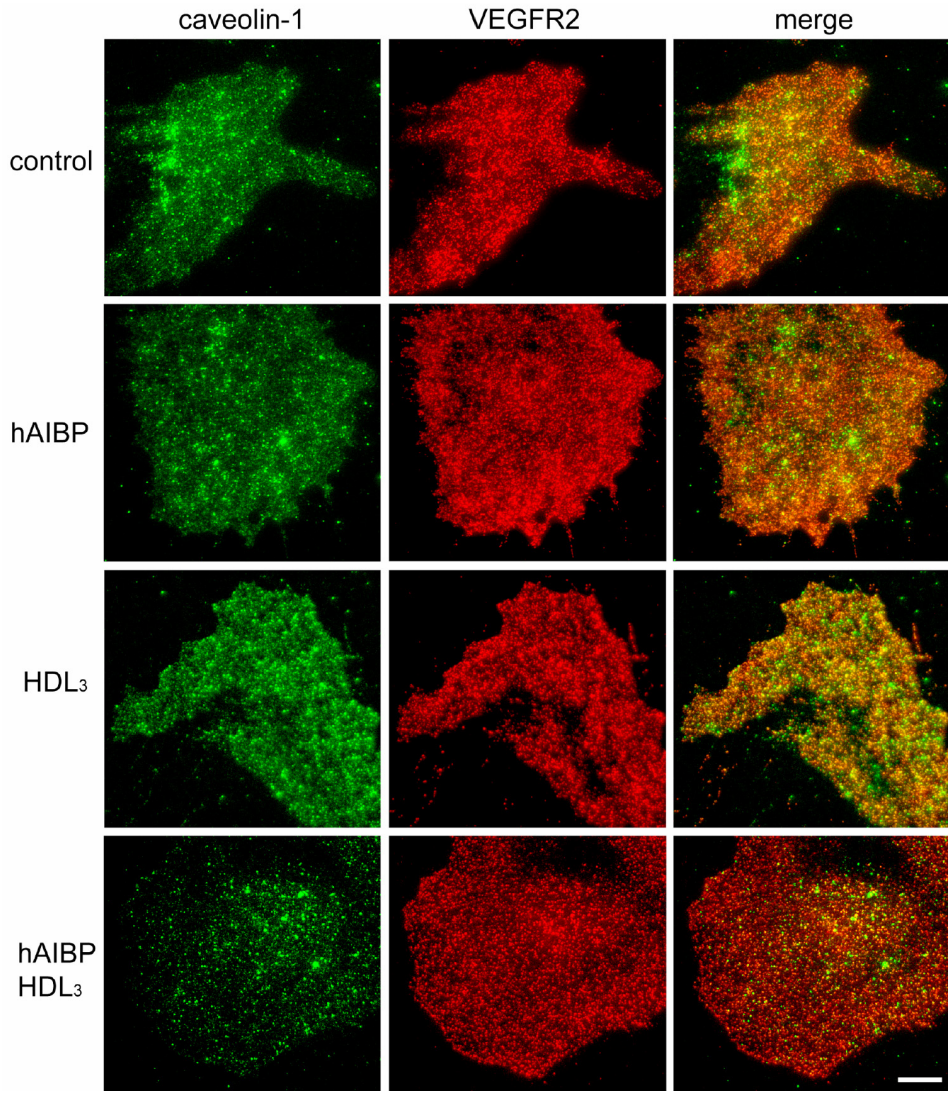
caveolin-1
VEGFR2
merge
control
hAIBP
HDL3
hAIBP
HDL3

b

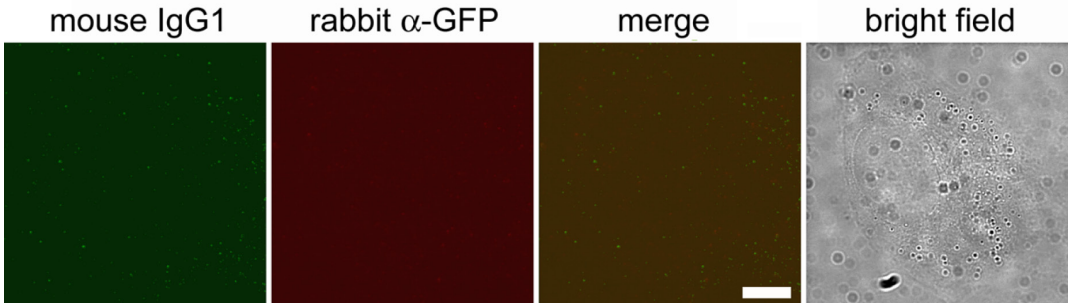
mouse IgG1
rabbit α-GFP
merge
bright field

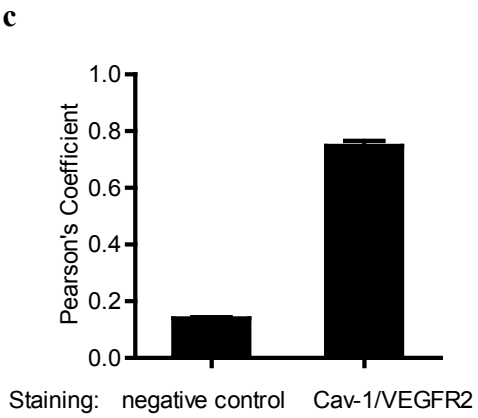

Supplementary Figure 6. Effect of hAIBP and HDL_3 on caveolin -1 and VEGFR2 surface localization. a, This supplementary figure is to illustrate the results shown on the graph of Fig. 2c. HUVEC were treated as in Fig. 2a, fixed and stained with antibodies to caveolin-1 (green) and VEGFR2 (red). Images were captured using TIRF microscopy. Scale, 10 μm. **b,** As a negative control, HUVEC were stained with a mouse IgG1 isotype (replacing the mouse caveolin-1 antibody) and a rabbit anti-GFP antibody (replacing the VEGFR2 antibody), followed by secondary antibodies. **c,** Accordingly, there was no colocalization of non-specific green and red signals as shown with Pearson's coefficient calculations.

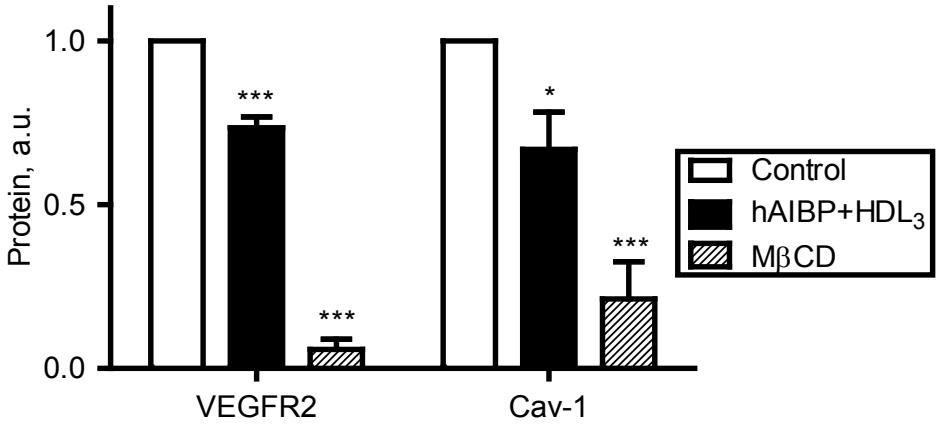

Supplementary Figure 7. Effect of hAIBP and HDL_3 on VEGFR2 and caveolin-1 localization to lipid rafts. This supplementary figure is the quantification of VEGFR2 and caveolin-1 in the lipid raft fraction (LR) shown in Fig. 2d. Equal protein amounts of each sample were loaded on gel. Mean±SD. The experiment was repeated 5 times for HDL_3+hAIBP and 3 times for MβCD treatments. *, $p<0.05$; ***, $p<0.001$.

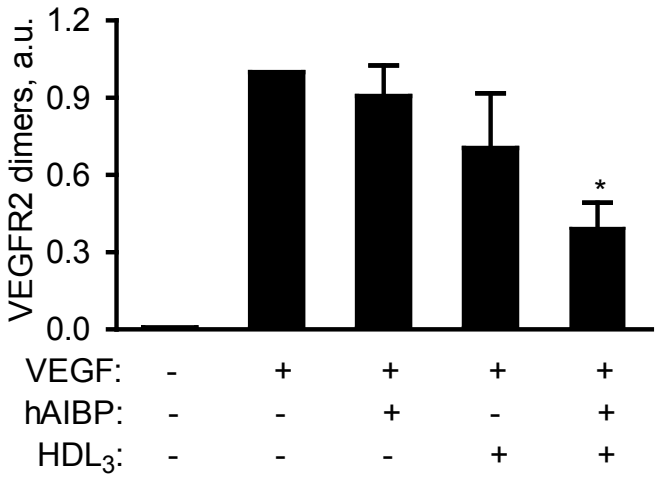

Supplementary Figure 8. Effect of hAIBP and HDL_3 on VEGFR2 dimerization. This supplementary figure is the quantification of the VEGFR2 dimerization experiment shown in Fig. 2e, calculated as dimer/(monomer+dimer). Mean±SD (n=3). *, $p<0.05$.

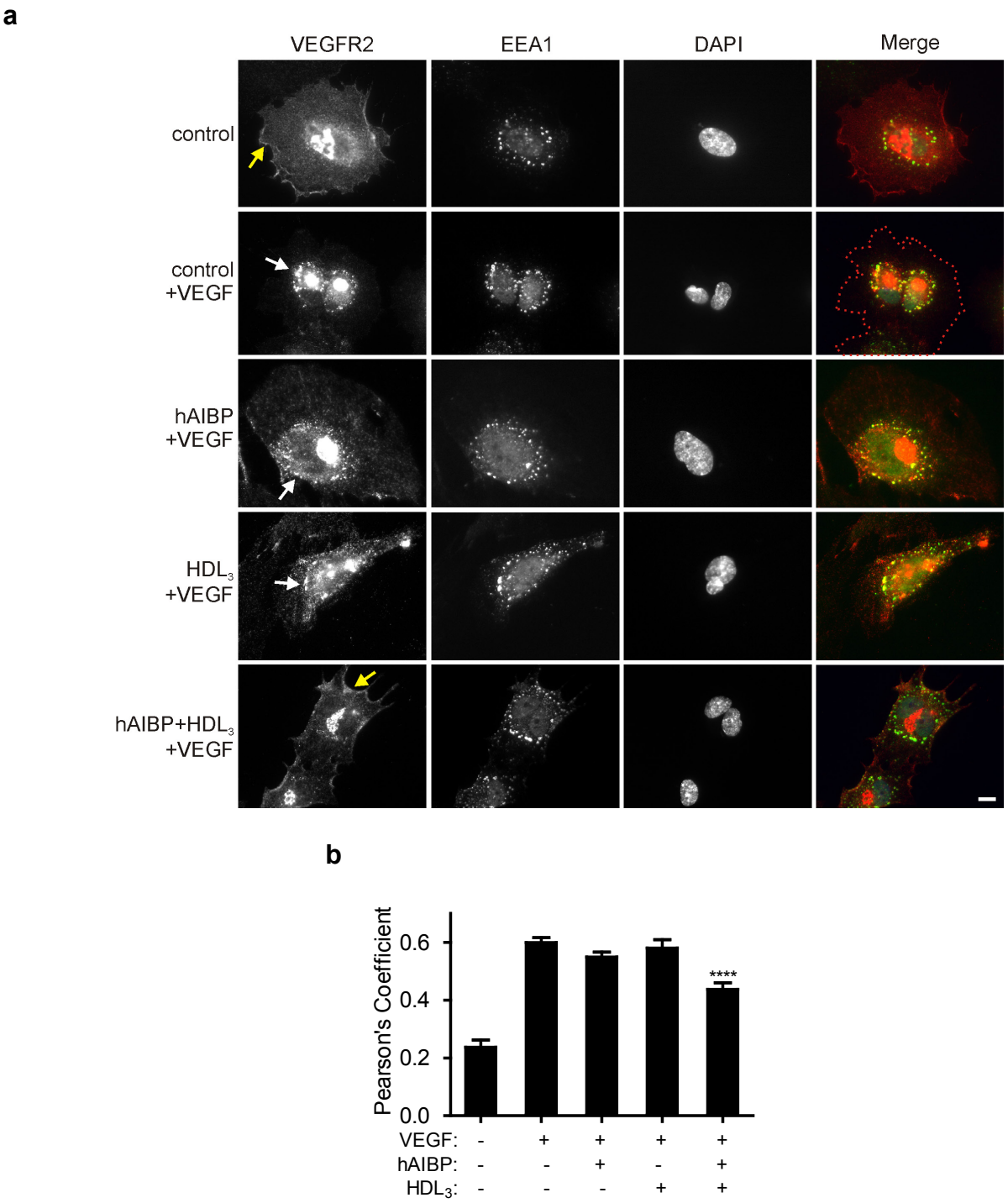

Supplementary Figure 9. Effect of hAIBP and HDL_3 on VEGFR2 endocytosis. This supplementary figure is an extension of Fig. 2f in the main text to show the results of additional treatment conditions. For that reason, the top two and the bottom row images in this supplementary figure are identical to the images in Fig. 2f. **a,** HUVEC were preincubated with 50 μg/ml HDL_3, 0.1 μg/ml hAIBP, or 50 μg/ml /ml HDL_3 + 0.1 μg/ml hAIBP for 4 hours, then stimulated with 50 ng/ml VEGF for 20 min, fixed and stained with antibodies to VEGFR2 (red) and the early endosome marker EEA-1 (green). Yellow arrows point to the surface localization of VEGFR2 and white arrows point to the endosomal localization of VEGFR2. Scale, 10 μm. **b,** The quantification of VEGFR2 and EEA-1 colocalization. Mean±SE (n=23 to 55). ****, $p<0.0001$.

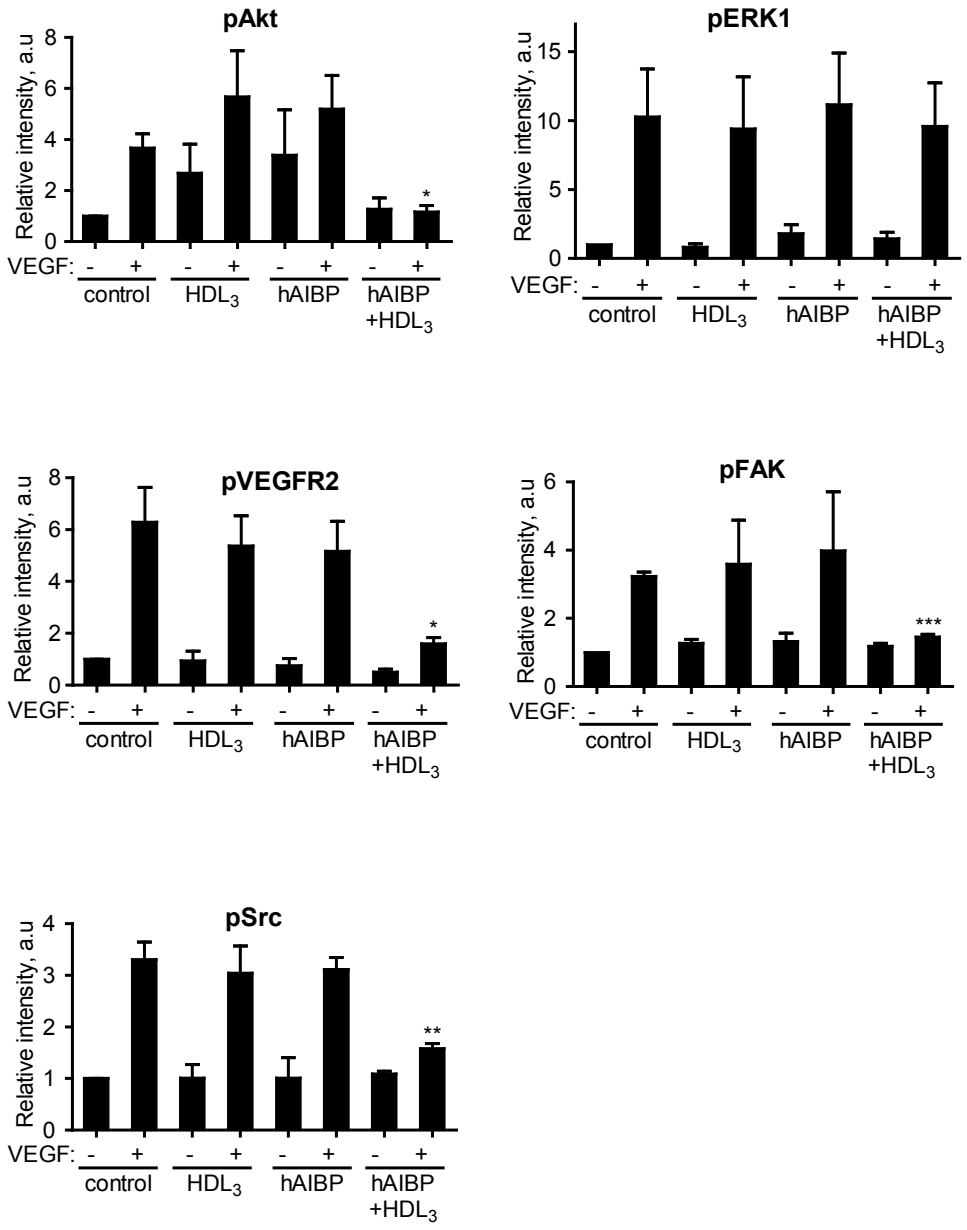

Supplementary Figure 10. Effect of hAIBP and HDL_3 on VEGF-induced signaling in HUVEC. This supplementary figure is the quantification of the signaling experiment shown in Fig. 2g. Normalized to β-tubulin and then to control (without VEGF). Mean±SD (n=3). *, $p<0.05$; **, $p<0.01$; ***, $p<0.001$.

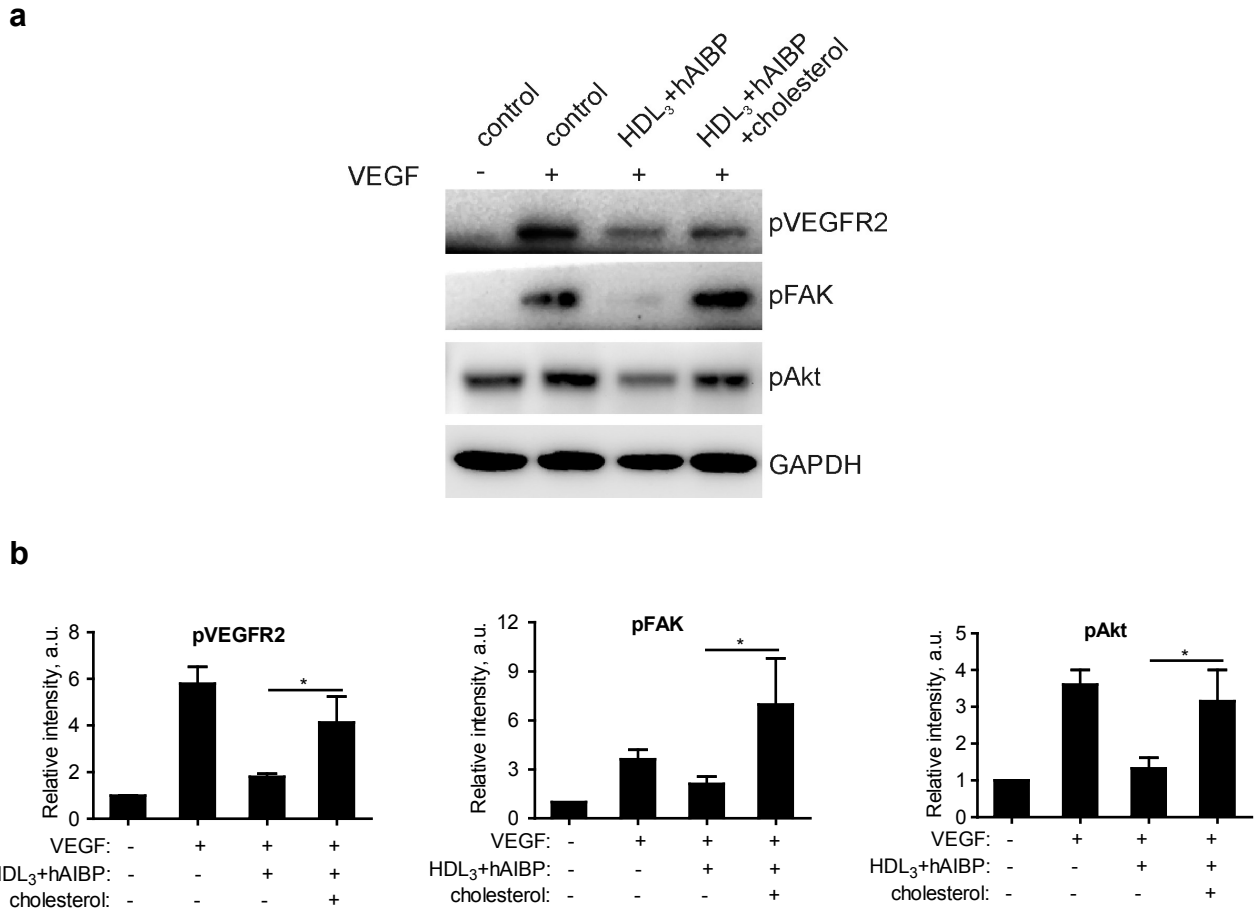

Supplementary Figure 11. Addition of cholesterol reduces the effect of hAIBP and HDL_3 on VEGF-induced signaling in HUVEC. a, HUVEC were preincubated with hAIBP and HDL_3 as in Fig. 2g, followed by a 1 hour incubation with or without 20 μg/ml cholesterol-MβCD. The cells were then stimulated for 20 min with 50 ng/ml VEGF, and cell lysates were run on SDS-PAGE, blotted and probed as indicated. **b,** The quantification of blot results. Normalized to GAPDH and then to control. Mean±SE (n=5). *, $p<0.05$.

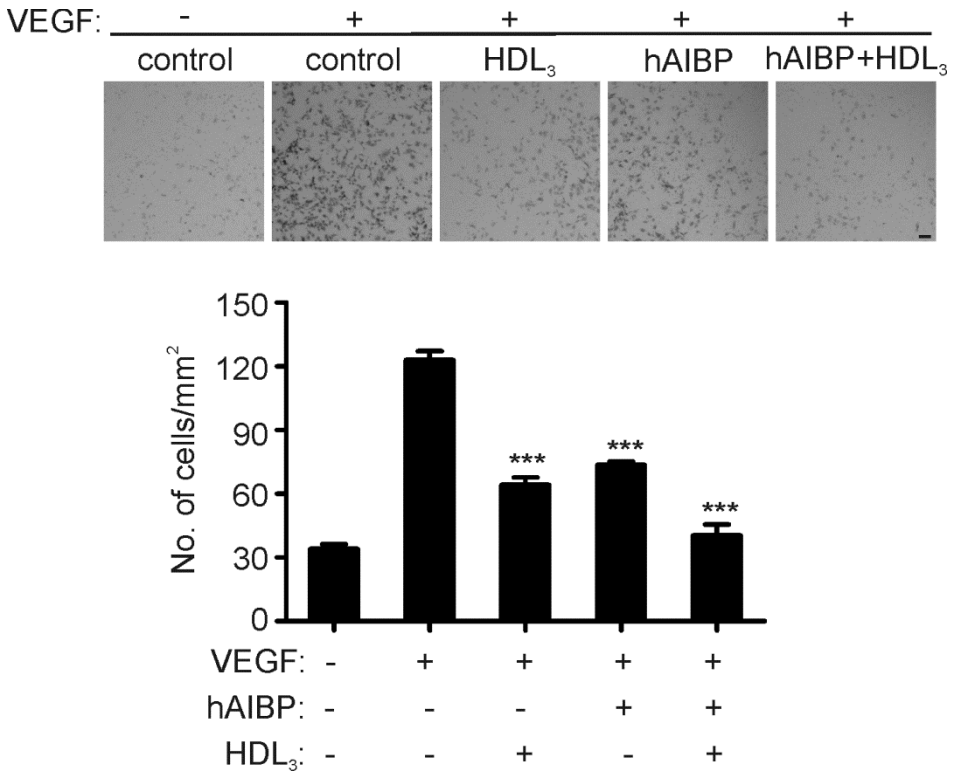

Supplementary Figure 12. Effect of hAIBP on VEGF-induced HUVEC migration. HUVEC, preincubated with 50 μg/ml HDL_3, 0.1 μg/ml hAIBP, or 50 μg/ml HDL_3 + 0.1 μg/ml hAIBP for 4 hours, were subjected to a migration assay as described in Methods. Mean±SE (n=5). ***, $p<0.001$.

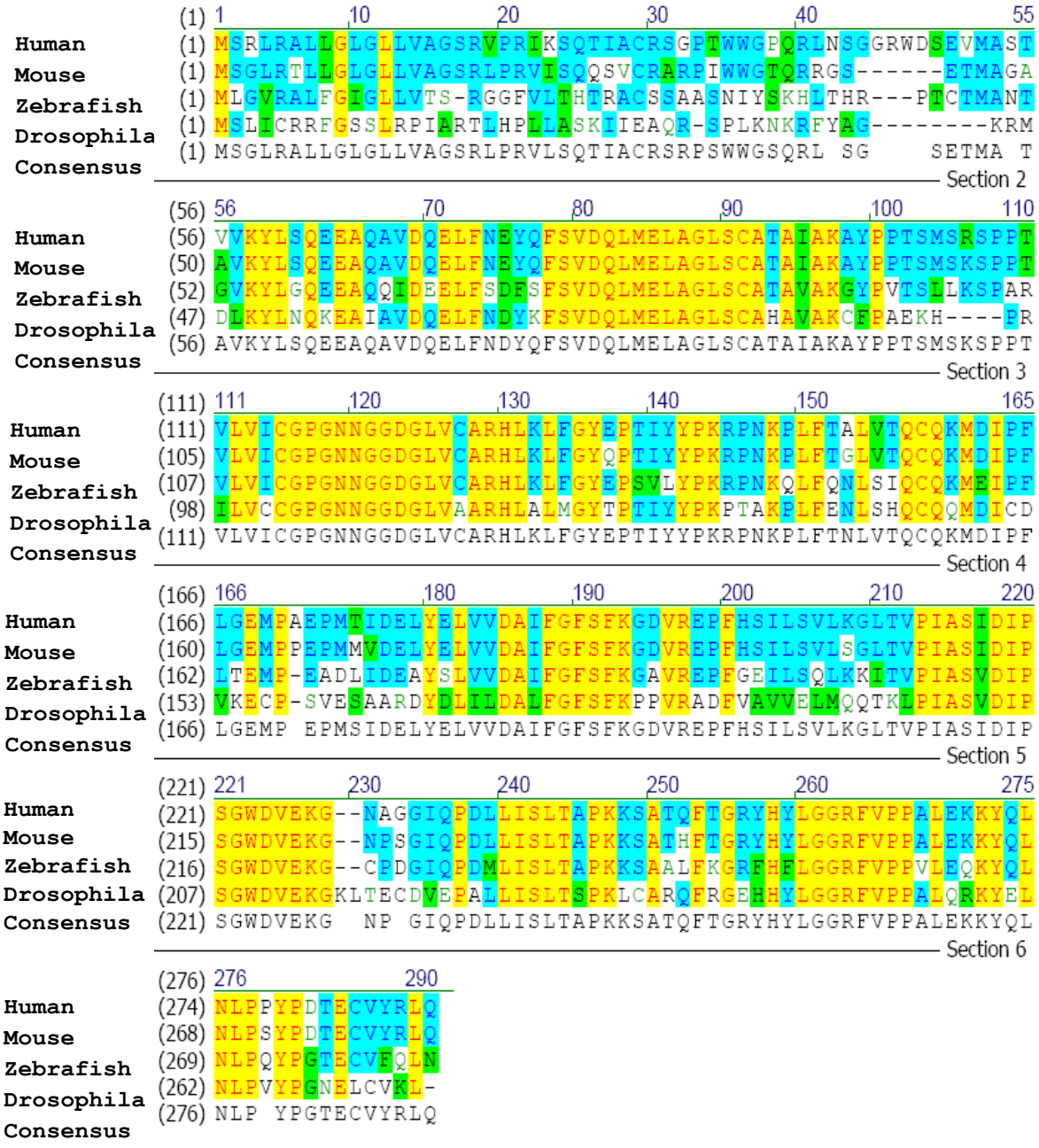

Supplementary Figure 13a. Conservation of AIBP proteins across different species. AIBP protein sequences were retrieved from ENSEMBL (http://uswest.ensembl.org/index.html) and were aligned using Vector NTI software (Invitrogen). Gene IDs of *AIBP* in different species: human *AIBP*: 128240; mouse *Aibp*: 246703; zebrafish *aibp1*: 436891. Drosophila *aibp*:CG2974-RB.

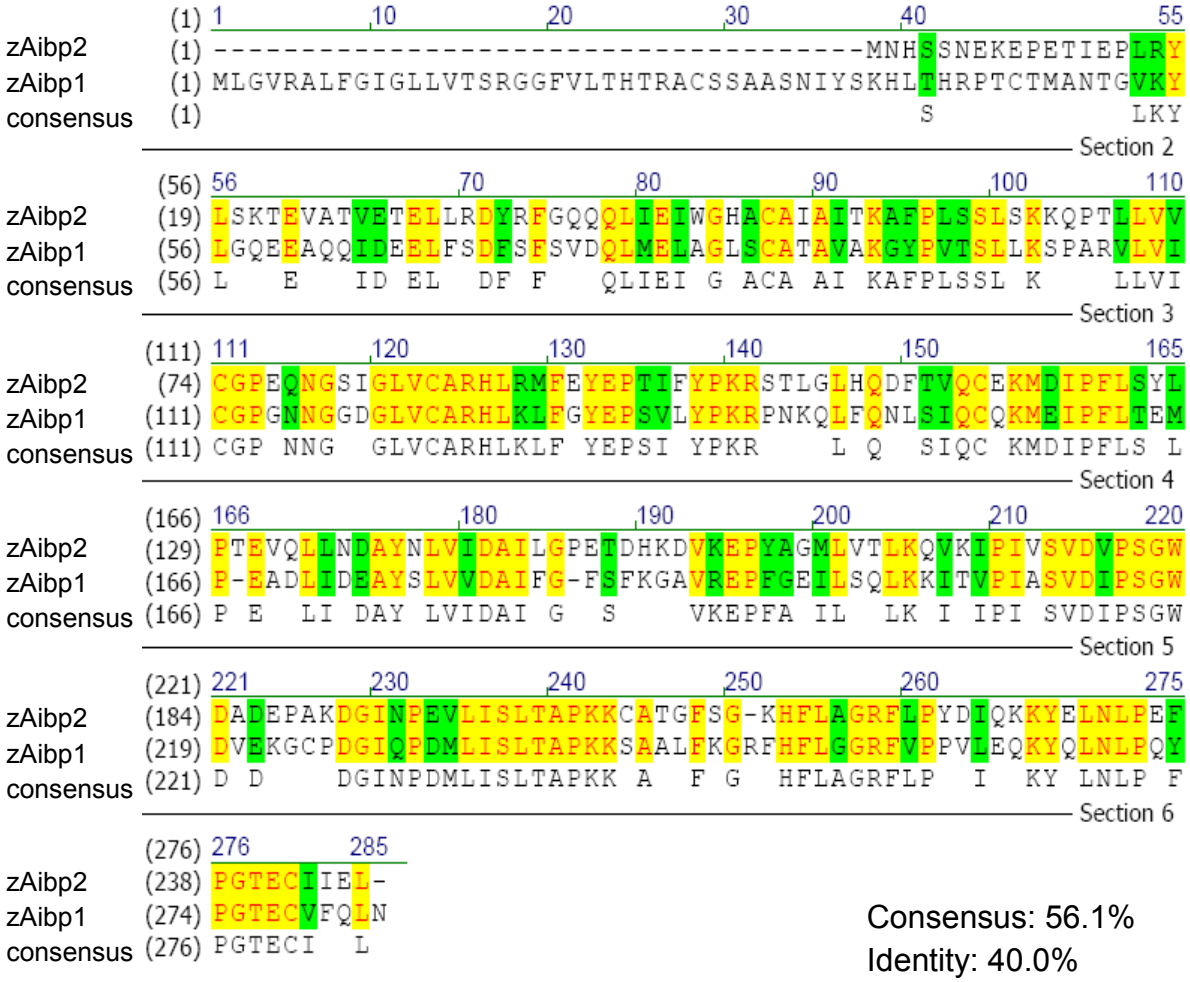

Supplementary Figure 13b. Two zebrafish AIBP proteins. Two AIBP isoforms originate from two different *zaibp* genes located on chromosomes 19 (*zaibp1*) and 22 (*zaibp2*). Comparisons were performed using Vector NTI software. Gene ID of zebrafish *aibp1*:436891; gene ID of zebrafish *aibp2*:557840.

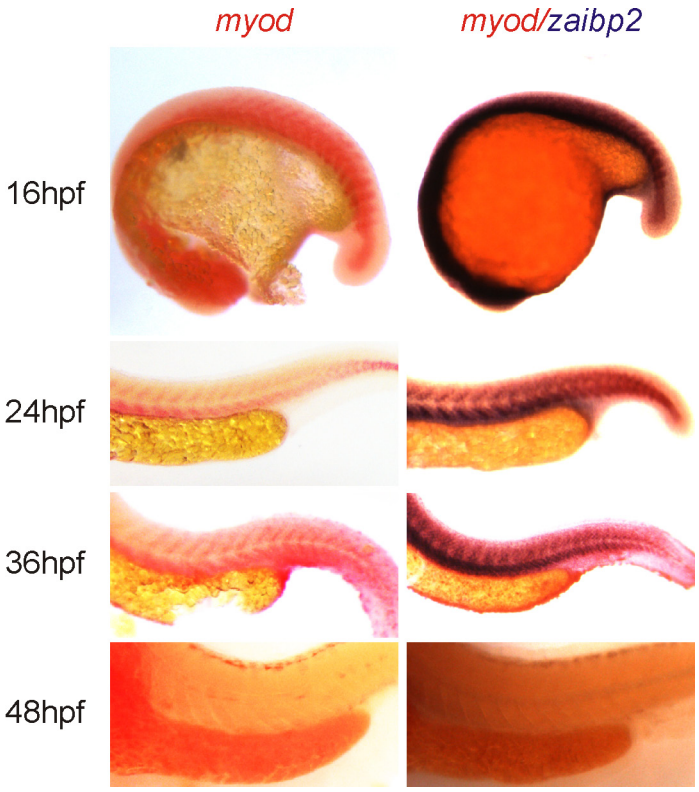

Supplementary Figure 14. Expression of *zaibp2* mRNA in zebrafish embryos at 16-48 hpf. The images in this supplementary figure are to supplement Fig. 3a, which shows only a 24 hpf time point.

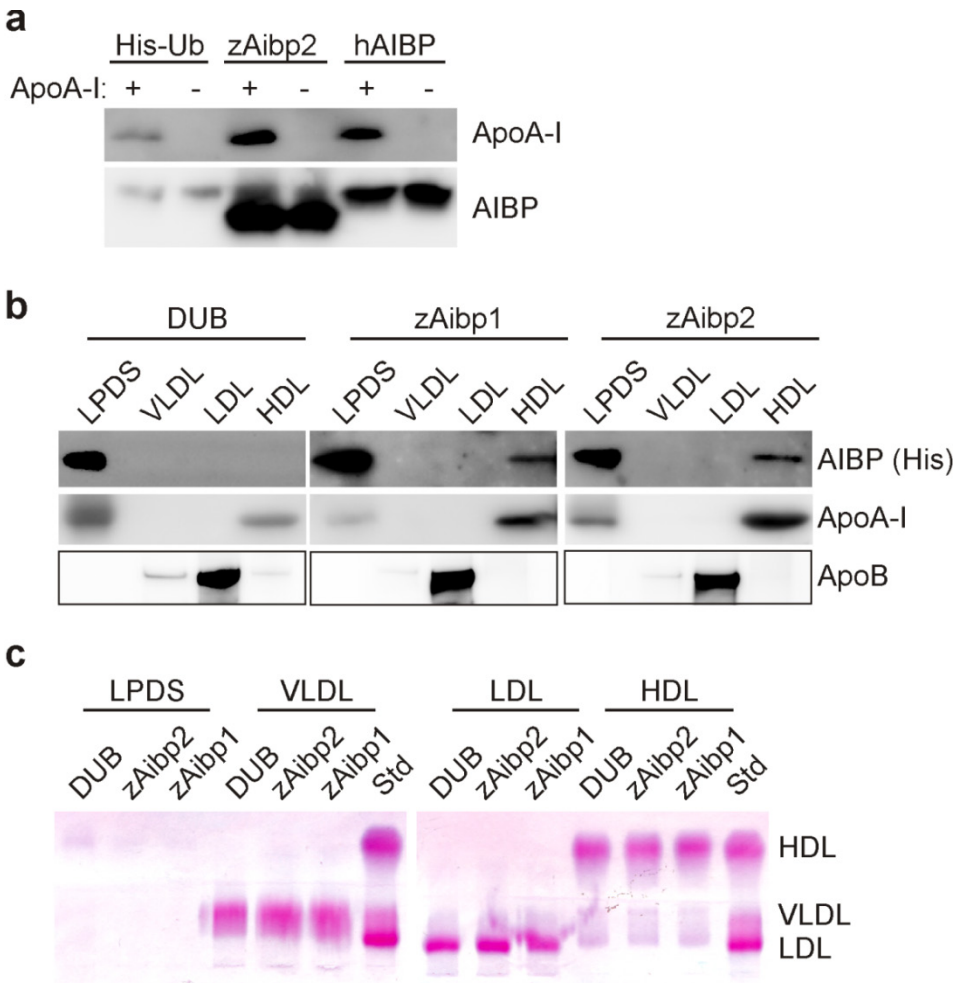

Supplementary Figure 15. zAibp binding to human ApoA-I. a, Three μg of purified human ApoA-I were mixed with 3 μg of His-tagged zAibp2 or hAIBP and then immunoprecipitated with an anti-His antibody. His-tagged ubiquitin was used as a negative control. The blots were probed as indicated. **b,** zAibp binding to human HDL. Five μg of purified His-tagged DUB, zAibp1 or zAibp2 were incubated with 1 ml of human plasma overnight at 4°C. Ultracentrifugation was performed to separate lipoprotein fractions. Different fractions of lipoproteins were run on SDS-PAGE and immunoblotted with indicated antibodies. **c,** Agarose gel electrophoresis of human lipoprotein fractions separated by ultracentrifugation, stained with FatRed. DUB, deubiquitinase; Std, human standard plasma; LPDS, lipoprotein-deficient serum.

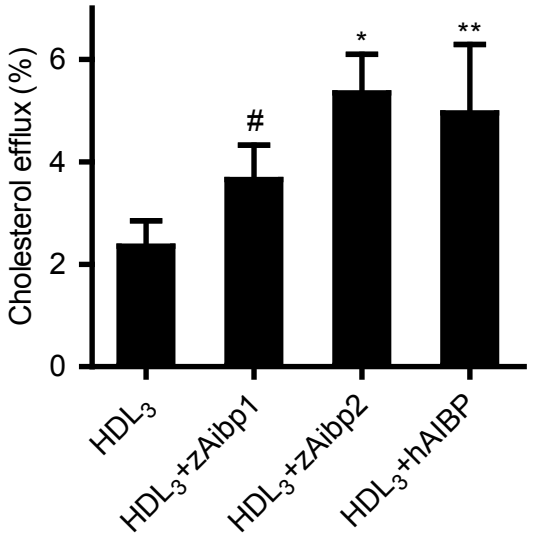

Supplementary Figure 16. Effect of zAibp on cholesterol efflux from HUVEC to HDL_3. HUVEC were preloaded with ^{3}H-cholesterol and then incubated for 1 hour with 50 μg/ml HDL_3 in the presence or absence of 0.2 μg/ml hAIBP, zAibp1 or zAibp2. The media and cell lysates were collected and ^{3}H counts were measured. Efflux was measured as the ^{3}H counts in the media divided by the sum of ^{3}H counts in the media and the cell lysates. Mean±SD; n=3. **, $p<0.01$; *, $p<0.05$; #, $p=0.08$.

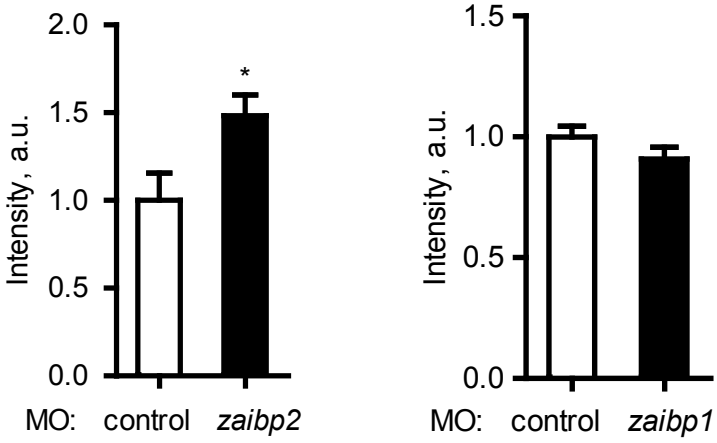

Supplementary Figure 17. Free cholesterol levels in *zaibp1* morphants. One-cell stage AB zebrafish embryos were injected with 8 ng of either control MO, *zaibp1* MO or *zaibp2* MO targeting ATG translation site. Twenty four hpf embryos were fixed and stained with filipin to detect free cholesterol in embryos. Intensities of filipin fluorescence in embryos (without yolks) were quantified. n=12-18. *, $p<0.05$.

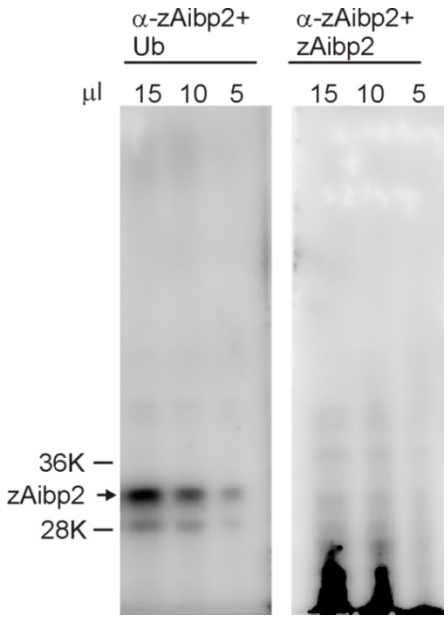

Supplementary Figure 18. Specificity of a zAibp2 antibody. A polyclonal antibody against zAibp2 (guinea pig post-immune serum) was used to probe zebrafish homogenates. Fifteen, 10 and 5 µl of the homogenates were loaded on an SDS gel, blotted and probed with the antibody, preincubated with 10 µg of either ubiquitine (Ub) or with zAibp2 (both recombinant proteins were produced from the same expression vector and under the same conditions). The blots were visualized with an anti-guinea pig IgG conjugated with HRP and a chemiluminescent substrate.

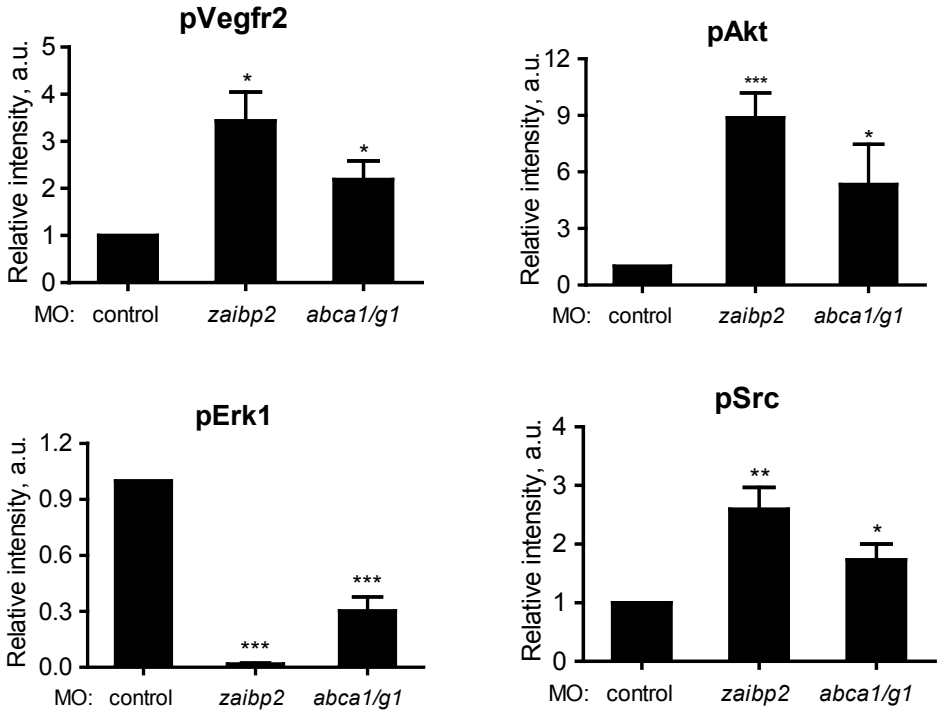

Supplementary Figure 19. Phosphorylation of signaling proteins in zebrafish lysates. This supplementary figure is the quantification of the immunoblot experiment shown in Fig. 3f. Erk1 is the p44 MAPK. There were no statistically significant differences in the pErk2 (p42) values. Normalized to β-tubulin and then to control. Mean±SD (n= 3 to 7). *, $p<0.05$; **, $p<0.01$; ***, $p<0.001$.

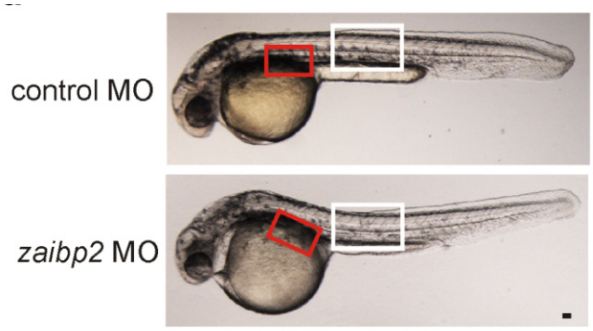

Supplementary Figure 20. Imaging areas. Low magnification, bright field images showing the area of fluorescent imaging of SeA (white box) and SIV (red box), which are displayed in Fig. 3g. Scale, 25 μm.

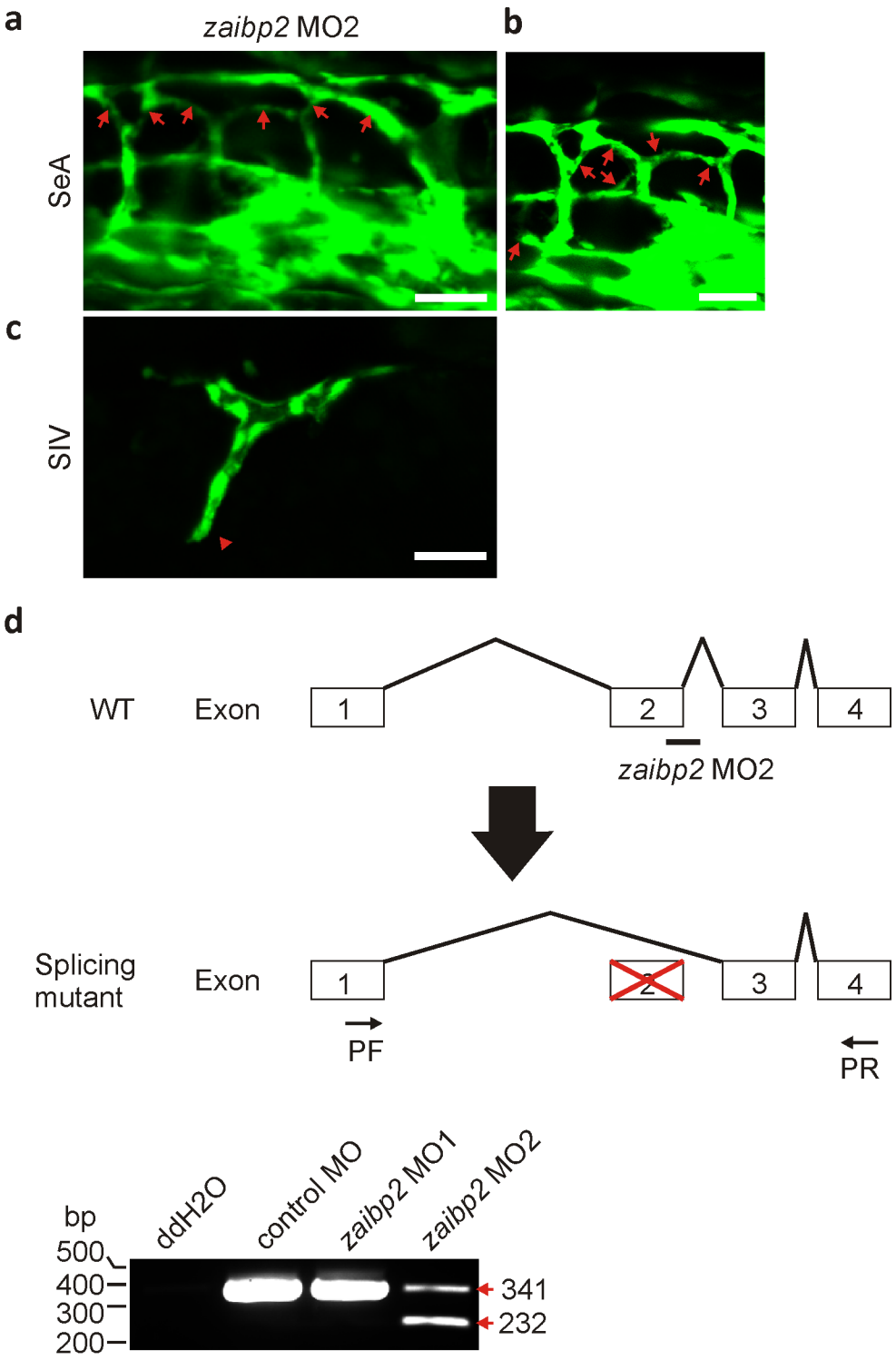

Supplementary Figure 21. Dysregulated SeA and SIV angiogenesis in *zaibp2* morphants (splicing site). a-c, One-cell stage *Tg(fli1:EGFP)* zebrafish embryos were injected with 8 ng of either control MO or *zaibp2* MO2, targeting a splicing site. The images of SeA (**a** and **b**) and SIV (**c**) were captured 3 days after MO injection. Arrows point to dysregulated sprouts. Scale, 50 μm. **d,** Diagram showing the targeted splicing site and gel showing corresponding PCR products. PF and PR indicate the primers used for the amplification.

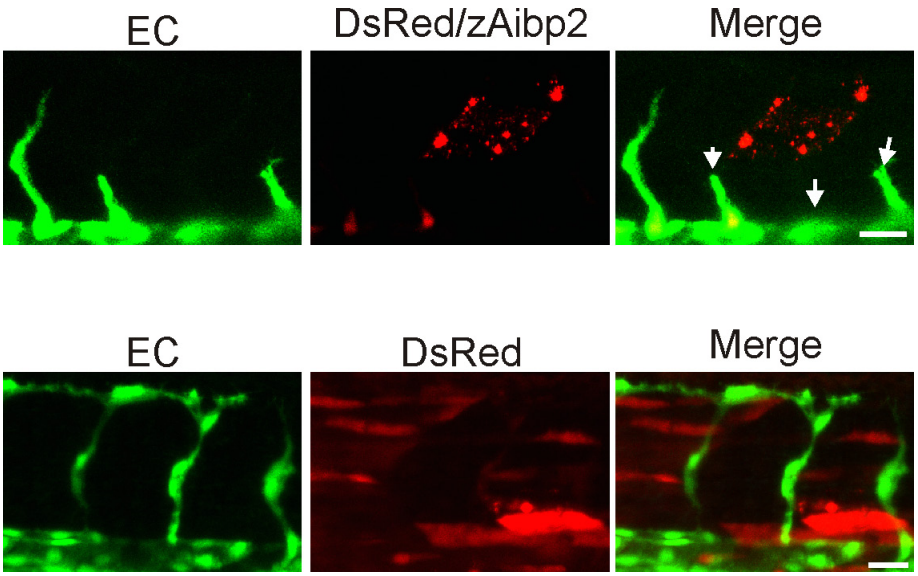

Supplementary Figure 22. Ectopic expression of zAibp2 inhibits SeA growth. One-cell stage *Tg(fli1:egfp)*^{y1} embryos were injected with 2 nl of 100 ng/µl DNA constructs for *myog:Gal4*, *DsRed:10×UAS:zAibp2* or *myog:Gal4*, *DsRed:10×UAS* expression. Images were captured at 30 hpf. Arrows point to aberrant SeA growth, close to the sites of DsRed (and zAibp2) expression. Scale, 25 µm.

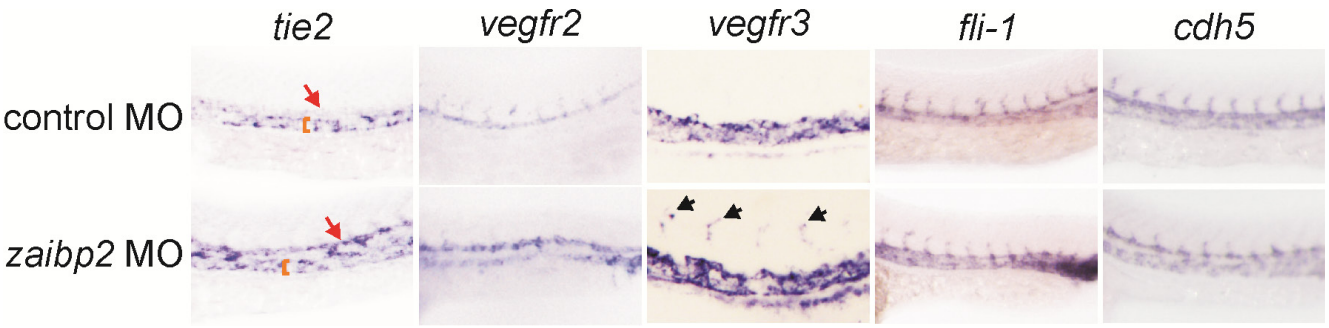

Supplementary Figure 23. **WISH analysis of genes involved in angiogenesis.** Twenty four hpf control and *zaibp2* morphants were fixed and hybridized with probes to *tie2* (GeneID:30747), *vegfr2/kdrl* (GeneID:796537), and *fli1* (GeneID:30619). A 28 hpf time point was used for *vegfr3/flt4* (GeneID:30121). *cdh5* (Gene ID: 445471) at 24 hpf was used as an internal control. Red arrows point to *tie2* expression in the dorsal aorta, and orange brackets show the posterior cardinal vein. Black arrows show increased expression of *vegfr3* in the SeA of a *zaibp2* morphant.

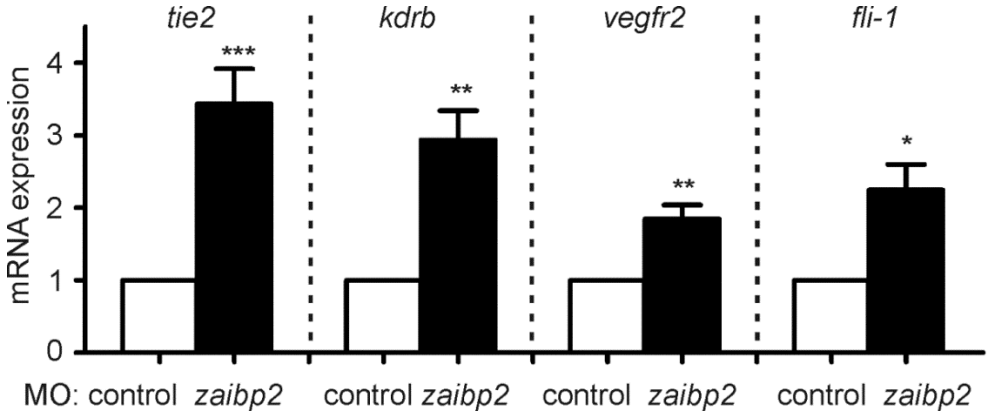

Supplementary Figure 24. **Expression of genes involved in angiogenesis.** Total RNA was isolated from 24 hpf control and *zaibp2* morphants and qRT-PCR was performed with primers for *tie2* (GeneID:30747), *kdrb*: (GeneID:554230), *vegfr2/kdrl* (GeneID:796537), and *fli1* (GeneID:30619). The mRNA levels were normalized to *β-actin* (Gene ID: 57934) mRNA and then to the values in control embryos. The results are from a pool of 50 embryos per group, 3-4 replicates.***, $p<0.001$; **, $p<0.01$; *, $p<0.05$.

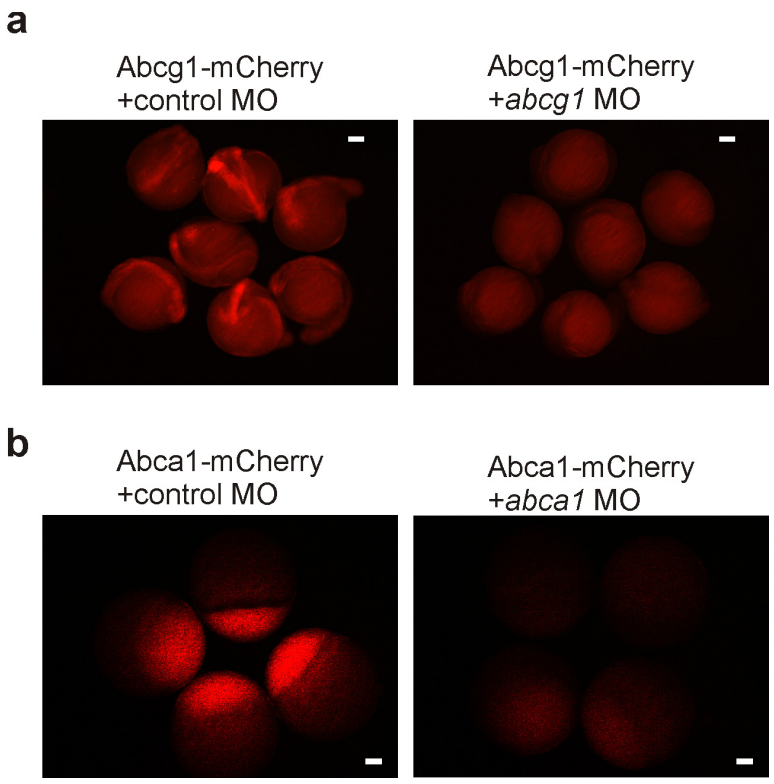

Supplementary Figure 25. Specificity of *abcg1* and *abca1* MOs. a, One-cell stage embryos were injected with mRNA encoding mCherry-tagged N-terminus of Abcg1, with control or *abcg1* MO. Images were captured at 12 hpf. **b,** One-cell stage embryos were injected with mRNA encoding mCherry-tagged N-terminus of Abca1, with control or *abca1* MO. Images were captured at 4 hpf. Scale, 100 μm.

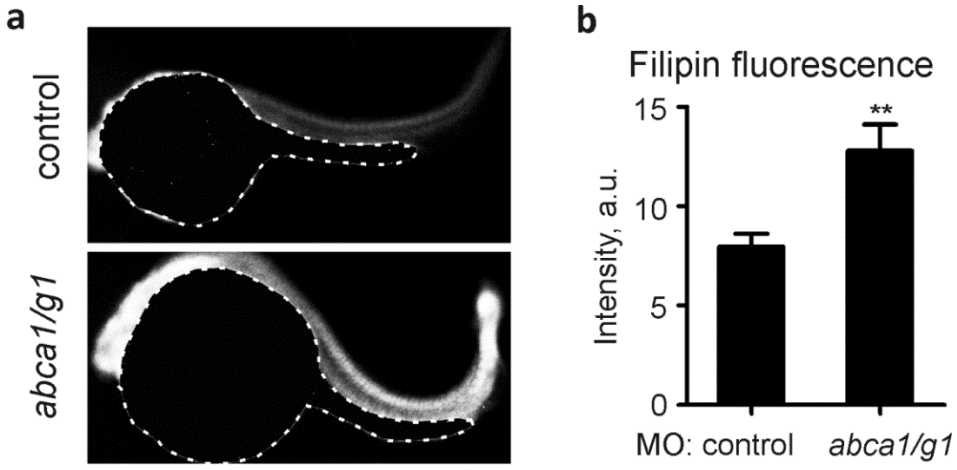

Supplementary Figure 26. Free cholesterol levels in *abca1/abcg1* morphants. a, Representative images of 24 hpf control and *abca1/abcg1* morphants stained with filipin to detect free cholesterol. Note the yolks are artificially masked. **b,** Intensity of filipin fluorescence in images shown in panel **a** (without yolks) was quantified in 8-10 embryos per group. **, $p<0.01$.

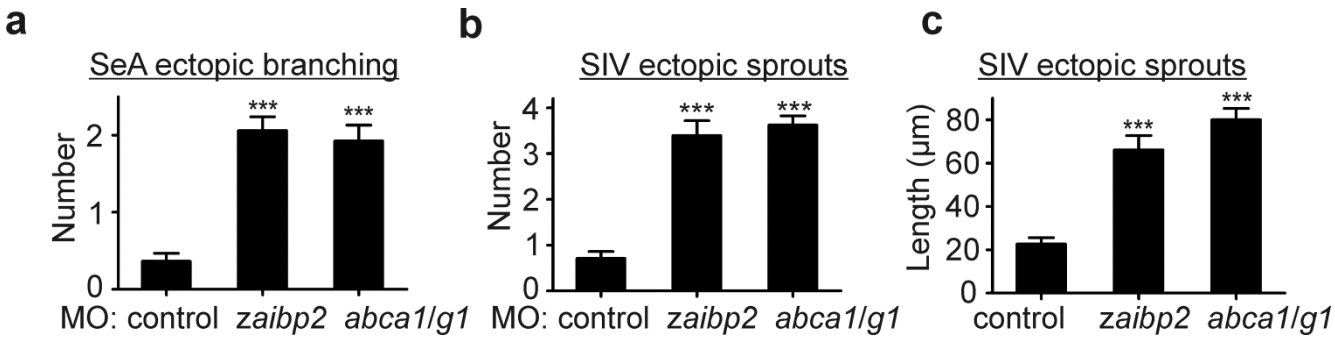

Supplementary Figure 27. **Quantitative data for Fig. 4c in the main text.** Graphs show numbers of SeA ectopic branches and numbers and length of SIV ectopic sprouts from 5-12 embryos.***, p<0.001.

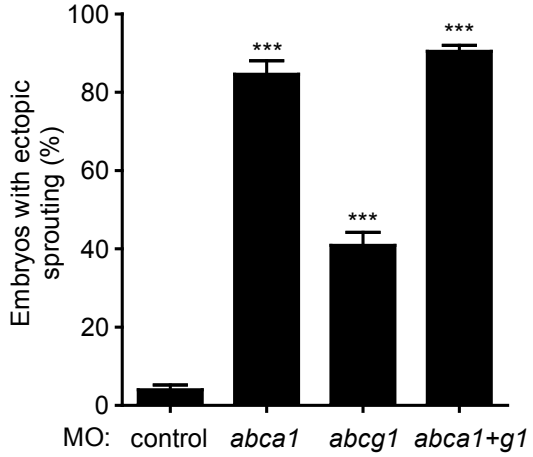

Supplementary Figure 28. Quantification of the number of embryos with normal and abnormal angiogenesis (SeA with ectopic branching) resulting from injection of 8 ng control, *abca1* or *abcg1* MO, or 4 ng *abca1* MO + 4 ng *abcg1* MO. 79-178 embryos per group. ***, p<0.001.